

**A Study of Some Measurement Errors  
in L2F-Velocimetry**

**F. Kost  
DLR Göttingen, Germany**

## **Summary**

In high speed flows the measurement accuracy of Laser-Two-Focus velocimetry is mainly determined by the statistical error due to insufficient number of sampled particles. Nevertheless there exist a lot of other sources of measurement error which may reduce the accuracy of the results: The geometry of the measurement volume leads to systematic errors in the turbulence degree. Windows which permit optical access to the internal flow may disturb the flow or distort the Laser measurement volume. The evaluation procedure may add some uncertainty. In the present study some of these measurement errors have been investigated numerically. In some cases systematic errors can be circumvented or may be corrected quantitatively. It can also be shown that measurement time may be reduced by choosing adequate parameters for the L2F-device and the measurement procedure, without affecting measurement accuracy.

## *Nomenclature*

$d$	effective diameter of L2F-focus
$s$	distance of the two L2F-focus
$u, v$	velocity components in cartesian coordinate system
$c$	velocity in polar coordinate system
$Tu$	turbulence degree
$\alpha$	angle (in radians)
$\varepsilon$	small quantity
$\varphi$	probability distribution function
$\sigma$	square root of variance, width of probability distribution
$N$	number of counts in a frequency distribution or number of particles traversing the start focus at a fixed angle
$n, n(\alpha)$	number of particles traversing the start <b>and</b> stop focus at a fixed angle

## **Subscripts**

$i$	index of measured event or $i$ -th angle
$b$	background (noise level) of a distribution
$u$	in direction of mean velocity vector
$v$	perpendicular to mean velocity vector
$\alpha$	flow angle distribution

## **Superscripts**

$--$	time mean value
$'$	deviation from mean value

## *Introduction*

To investigate the flow field inside turbomachine components the Laser-Two-Focus velocimeter (L2F) is an appropriate tool. A detailed description of a L2F-velocimeter was given by Schodl [1]. The L2F-measuring device generates two highly focussed light beams in the probe volume which act as a 'light gate' for tiny particles in the flow. The scattered light from the particles provides two successive pulses and from the time interval between the pulses the velocity perpendicular to, but in the plane of the laser beams can be derived. The mean flow angle is provided by turning the second beam around the first and so accumulating time-of-flight histograms at a number of angles.

The L2F device has several advantages making it especially useful for measurements in turbomachinery components, but the measurement procedure is rather time consuming. In the past years a number of L2F-measurements have been conducted in the

windtunnel for rotating annular cascades at DLR Göttingen [2]. One conclusion from those measurements was that it is very important to have an error bar available for each measured quantity at any point. There is furthermore a strong demand to reduce measurement time (to improve measurement efficiency).

In the following sections some measurement errors (not all) of the L2F measurement procedure and evaluation will be described. Furthermore some suggestions are made concerning measurement efficiency.

### *Numerical simulation of a Laser-Two-Focus measurement*

Some years ago, when 'L2F' was still a rather new instrument, there was not much information available, concerning the intrinsic measurement error of the L2F-device. This led to the intention to create a numerical program which enabled us to simulate the L2F-measurement. It is not a surprise that other persons had the same idea [3, 4]. Our program proved to be especially useful when testing the L2F evaluation program and also at the beginning of the development of the 3D-L2F prototype [5].

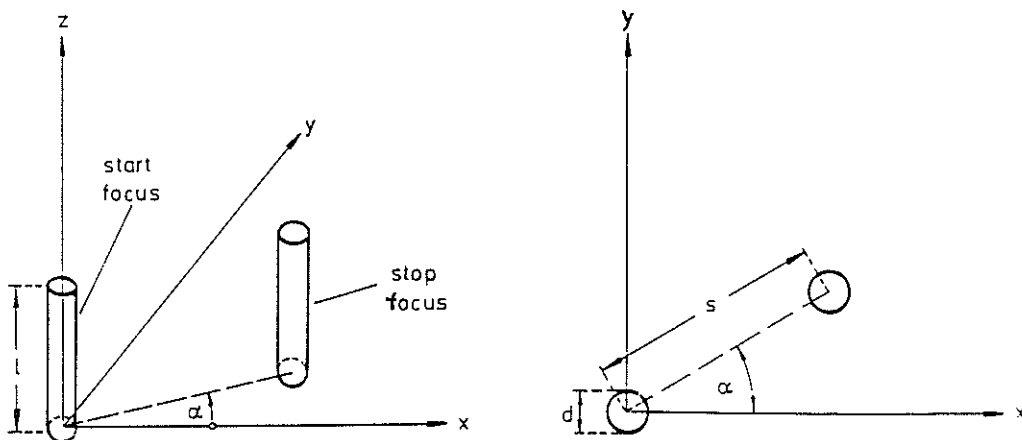


**Figure 1. Measurement volume for the numerical simulation**

The L2F measurement volume for the numerical simulation consists of two cylinders as shown in **Figure 1**. Start focus is a cylinder of a certain length parallel to the z-axis and located at the origin. The stop focus is also parallel to the z-axis but it is located at a distance  $s$  from the start focus and at an angle  $\alpha$ . In order to simulate a real L2F measurement the program proceeds in the following way:

- 3D velocity vectors are generated with the aid of a random number generator. The velocity components are normally distributed, they possess a mean value, a variance and a correlation, according to a given fully 3D Reynolds' stress tensor.
- The start-focus is divided into many patches.
- A particle possessing a 3D velocity starts in a patch of the start focus, the program looks, whether the stop focus is hit, it computes the flight time and stores the event.
- After a certain number of started particles the patch in the start cylinder is changed, after using all patches the angle of the stop focus relative to the start focus is changed and the previous steps are repeated. In z-direction the particles may also have different mean velocity values.

When using such a simulation it is assumed that the single velocity vectors are random values but the velocity components are distributed according to a 3D Gaussian or normal distribution. The 'successful measurement events' of the simulation are stored in the same way as the L2F device does it, i.e. as time-of-flight distributions. To these distributions background noise may be added finally. To test a L2F-evaluation program the resulting distributions were passed to the evaluation program. To look for statistical errors only a limited number of particles were started in the start focus. If there was interest in systematic errors of the measurement procedure, the so-called intrinsic errors, then numerous particles were started to make the statistical errors small.

The above described program does not allow to simulate the stochastic arrival of the particles in a real measurement which leads to the so-called 'statistical bias', but nearly all other characteristic features of a L2F measurement can be correctly simulated.

Taking a cylinder as start and stop focus is the most questionable assumption in the simulation and throughout this whole paper. For example, in the appendix it is shown that a plane glass window may lead to a shape of the focus which is very far from a cylinder or anything else having axisymmetry, if the axis of the light beam and the vertical on the window deviate much. A certain freedom is introduced in the simulation program as the diameter and the length of the cylinder may be chosen as independent parameters and it is possible to use subsequently cylinders of different diameters and lengths during one simulation, adding all successful events from the different cylinders.

Another basic assumption is that a particle passing a cylinder is always detected by the optics when traversing the inside of the cylinder, but it is not detected when remaining outside. That means the detection function is a step function and not a Gaussian distribution or something else. This special feature is justified by following

arguments: In high speed gas flows incoming particles are not so abundant that they compete for detection. They are detected when they scatter a sufficient amount of light into the direction of the detector. The amount of scattered light is a function of particle size and light amplitude in the focus. If there is not too much variation in particle size then it is certainly possible to define an effective focus diameter (and length) which depends on the special detection optics and electronics but is nevertheless constant during a fixed setting of the device.

This paper confines itself to flows with turbulence degrees less than 16%. For such flows the exact length of the L2F focus is of minor importance compared to the effective diameter, as the focus diameter is much smaller than the focus length. That is why in the following simulations the length was always kept constant and only the diameter and the distance of start and stop cylinder varied which means that in this investigation 3D effects did not play a role.

### *Statistical error*

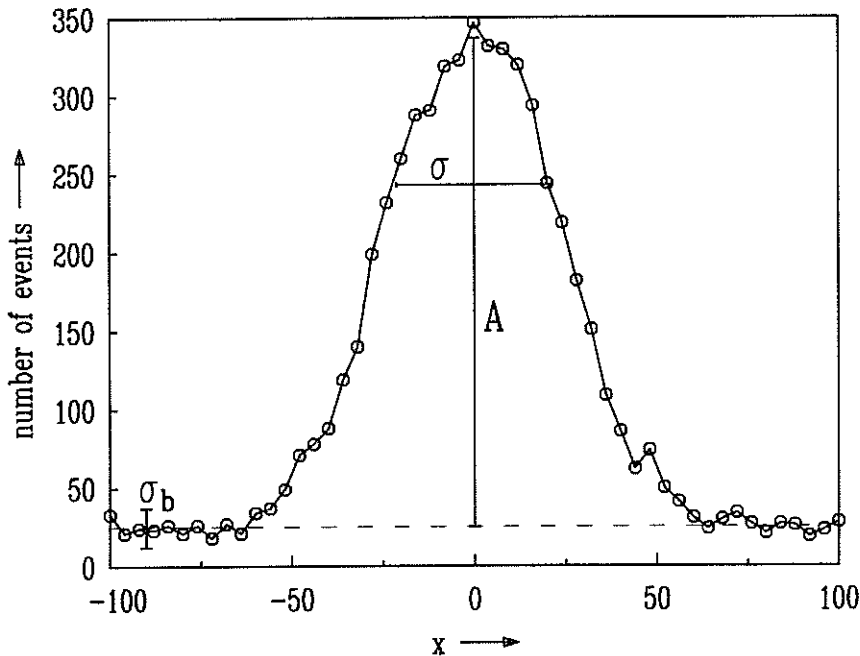


Figure 2. Frequency distribution with background noise added

In **Figure 2** a typical frequency distribution is shown, approximating a normal distribution of amplitude  $A$  and variance  $\sigma^2$ . At the base of the normal distribution a background noise level has been added. The amplitude of the background noise has

the variance  $\sigma_b^2$ . This distribution resembles a measured distribution of frequency versus velocity or frequency versus angle (a distribution which results from integrating the frequencies in the time-of-flight distributions at fixed angle).

It is a common problem to compute the mean and the variance of the quantity  $x$  from such a noisy distribution. By the numerical simulation program a number of such distributions with different total numbers of events,  $N_{total}$ , in the distribution and different background levels were produced. From each distribution the mean was computed and compared with the exact mean. From the whole sample one could then derive a formula relating the error to the decisive parameters. The constant in the formula was computed by a 'Least Square Fit'. A similar problem was investigated analytically by Bobroff [6]

$f_{\bar{x}}$  = error of the mean  $\bar{x}$  (95% confidence interval) .

$$f_{\bar{x}} = \frac{2\sigma}{\sqrt{N}} \cdot \sqrt{1 + c \cdot \frac{\sigma_B^2}{\Lambda}} ; \quad \frac{\sigma_B^2}{\Lambda} < 0.9$$

1. evaluation of distribution in the region  $\bar{x} \pm 3 \sigma$   
( $N = 99.7\%$  of  $N_{total}$ ) :  $c \approx 10$
2. evaluation of distribution in the region  $\bar{x} \pm 2 \sigma$   
( $N = 95.5\%$  of  $N_{total}$ ) :  $c \approx 4$

The form of the above equation was of course chosen in such a way that without background noise,  $\sigma_B = 0$ , just the commonly known statistical error  $2\sigma / \sqrt{N}$  results. The sample from which the constant  $c$  in the above equation was computed, was not large. That is why the constant  $c$  could be only approximately determined. Nevertheless it can be seen that the background noise influences the error  $f_{\bar{x}}$  differently: When the 'whole' distribution is evaluated (case 1) the influence is much bigger than in case 2, where the outer part of the distribution was ignored when computing the mean.

The practical importance for L2F measurements is two-fold: First we have an equation from where we get an error bar for the measured quantity. Secondly, the above result tells us that it is not desirable to cover the whole distribution during a measurement. Especially the angle range of the L2F measurement need not cover the whole flow angle distribution, so saving measurement time without increasing the error.

*Evaluation error when using only integrated distributions*

Schodl [1] suggested a L2F measurement procedure which ought to reduce measurement time by storing only the integrated time-of-flight and angle distributions. In **Figure 3** two equal two-dimensional frequency distributions and the related one-dimensional integrated distributions are shown. The usual definition of the mean flow values  $\bar{u}$ ,  $\bar{v}$ ,  $Tu_u$ ,  $Tu_v$  (see below), would require to integrate the 2D distribution in cartesian coordinates. By storing only the integrated time-of-flight and angle distributions an implicit integration in polar coordinates is performed. This leads to a systematic error which has to be minimized.

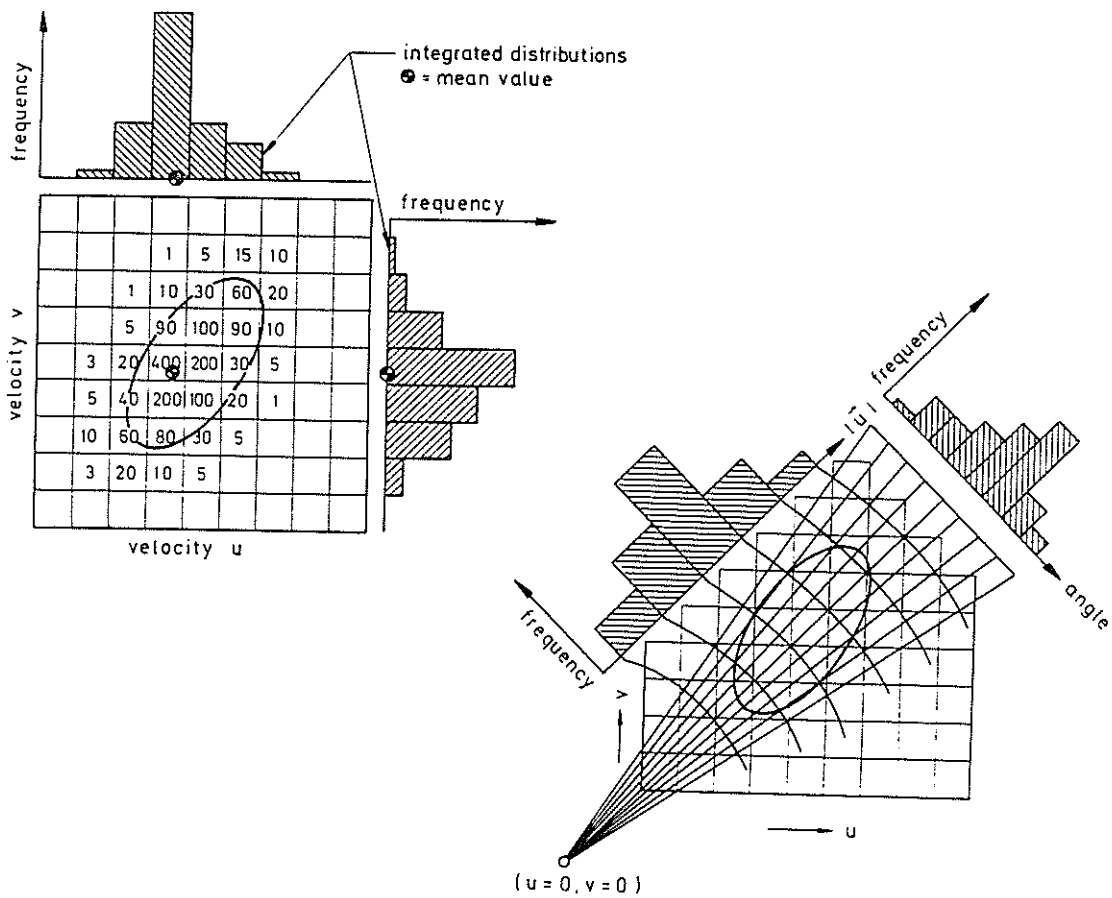


Figure 3. Frequency distribution in a cartesian and a polar coordinate system

The coordinate system is oriented in such a way to give  $\bar{\alpha} = 0$

velocity-components in cartesian coordinate system:  $u, v$

velocity, angle in polar coordinate system:  $c, \alpha$



mean values in cartesian system

$$\bar{u} = \frac{1}{N} \sum_{i=1}^N u_i$$

$$\bar{v} = \frac{1}{N} \sum_{i=1}^N v_i$$

$$u'_i = u_i - \bar{u}$$

$$v'_i = v_i - \bar{v}$$

$$\overline{u'^2} = \frac{1}{N-1} \sum_{i=1}^N u'^2_i$$

$$\overline{v'^2} = \frac{1}{N-1} \sum_{i=1}^N v'^2_i$$

mean values in polar system

$$\bar{c} = \frac{1}{N} \sum_{i=1}^N c_i$$

$$\bar{\alpha} = \frac{1}{N} \sum_{i=1}^N \alpha_i$$

$$c'_i = c_i - \bar{c}$$

$$\alpha'_i = \alpha_i$$

$$\overline{\cos \alpha'} = \frac{1}{N} \sum_{i=1}^N \cos \alpha'_i$$

$$\overline{\sin^2 \alpha'} = \frac{1}{N} \sum_{i=1}^N \sin^2 \alpha'_i$$

The quantities  $\bar{u}, \bar{v}, \overline{u'^2}, \overline{v'^2}$  have to be approximately computed from  $\bar{c}, \overline{c'^2}, \overline{\cos \alpha'}, \overline{\sin^2 \alpha'}$ .

There is:  $\alpha_i \ll 1$  and  $\frac{c'_i}{\bar{c}} \ll 1$ .

$$u_i = c_i \cos \alpha_i \Rightarrow$$

$$\bar{u} \approx \bar{c} \cdot \overline{\cos \alpha'} + o(\varepsilon^3) \quad (1)$$

$$v_i = c_i \sin \alpha_i \Rightarrow$$

$$\bar{v} \approx 0 + \overline{c' \alpha'} + o(\varepsilon^4) \quad (2)$$

$$\Rightarrow \bar{v} \approx 0 + \frac{\overline{u' v'}}{\bar{u}}$$

$$\sigma_u^2 \approx \overline{c'^2} - \overline{c'} \overline{c'\alpha'^2} + o(\varepsilon^4) \tag{3}$$

$$\sigma_v^2 \approx \overline{c'^2 \sin^2 \alpha'} + 2\overline{c'} \overline{c'\alpha'^2} + o(\varepsilon^4) \tag{4}$$

In the above equations always the first term on the right side can be derived from the integrated distributions in the polar system. The remaining terms denote the systematic error introduced by integrating the 2D distributions in polar coordinates instead of in a cartesian coordinate system.

As an example the mean velocity  $\bar{v}$  is given the value zero, but in reality it should have  $\overline{u'v'}/\bar{u}$ . Or, the Reynolds' stress determines the error of  $\bar{v}$  to first order. The above derivation did not use a specific L2F feature. That means any measurement device which delivers a mean value in a polar coordinate system, for example by determining a mean angle, gives the same error.

In the following figures the errors of the resulting turbulence degrees are plotted.

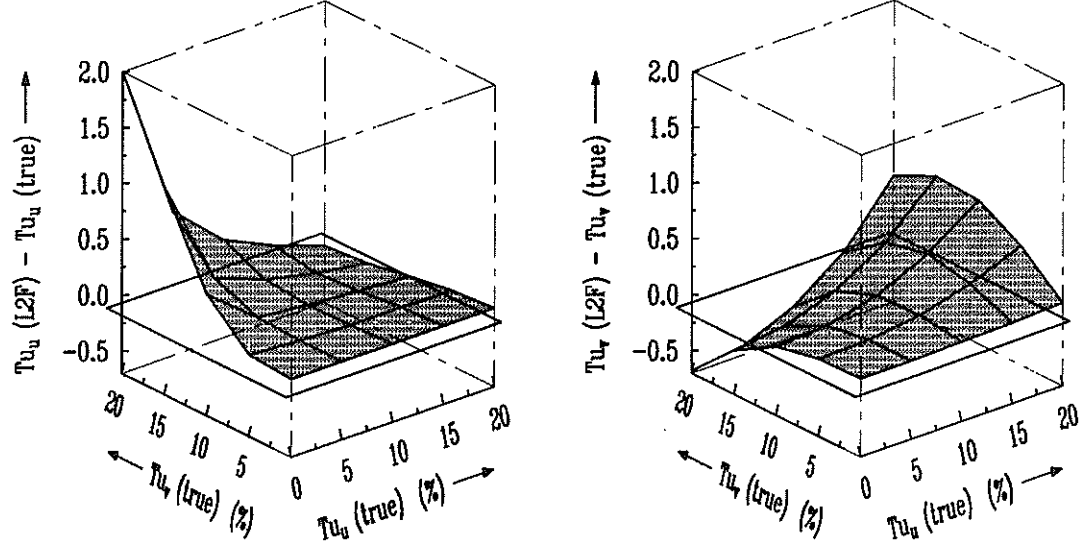


Figure 4. Error of turbulence degree (error surfaces), correlation  $r = 0$

In **Figure 4** error surfaces are shown for the case of no correlation between the variance of the u- and v-component.

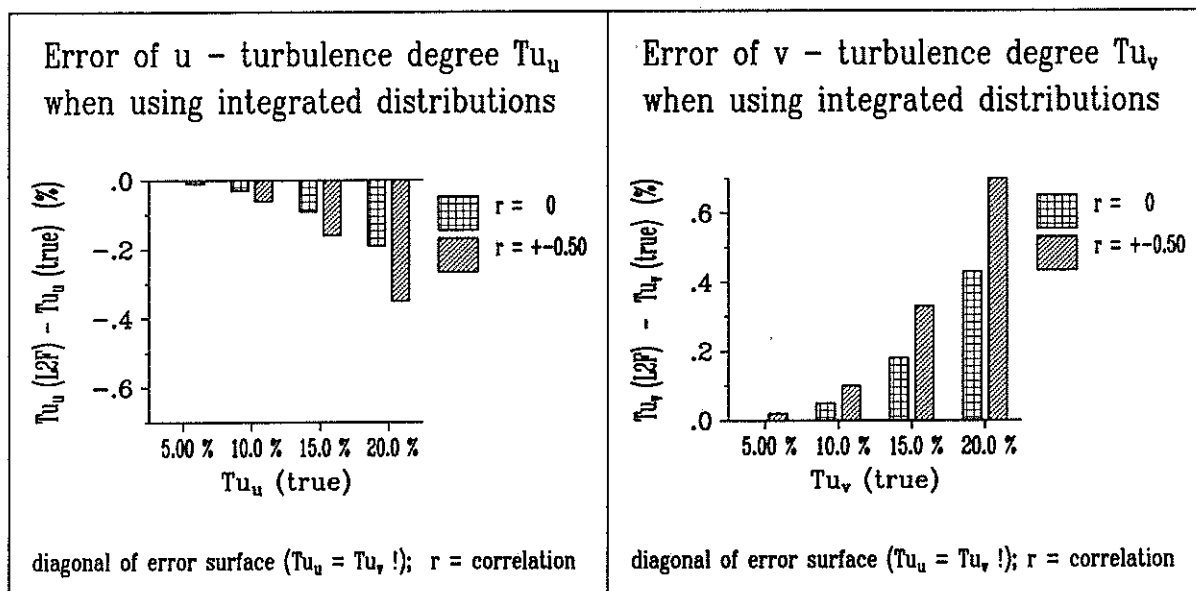


Figure 5. Error of turbulence degree (diagonal of error surface)

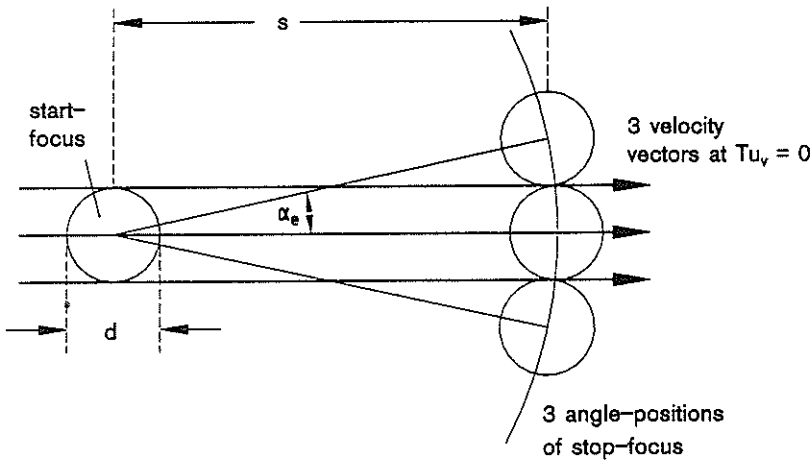
In **Figure 5** the diagonal of the error surfaces are shown, but the case of a correlation between u- and v-component is included.

The errors resulting from these integrated distributions are normally smaller than the statistical error. Nevertheless it is desirable to avoid the use of the integrated distributions in the future because the integration procedure by summing up the events in a time-of-flight and angle distribution strictly requires that scattered light from surfaces is independent of the angle setting. This requirement cannot always be fulfilled especially when measurements near to surfaces are performed.

### *Error in measured turbulence degree coming from the finite diameter of the focus*

Because of finite diameter of the L2F focus, measurement events occur even then, when the angle of the stop focus is such that no particles from the start focus should hit the stop focus. The finite diameter of the two focus leads to angle distributions which are too wide and so a too high turbulence degree  $Tu_v$  results. The following analysis uses the assumptions concerning the focus stated above, that are: cylindrical focus and existence of an effective focus diameter. A strongly distorted focus, as described in the appendix, would lead to different results.

According to **Figure 6** a triangle-shaped angle distribution would be measured when the turbulence degree  $Tu_v$  is approximately zero.



Measured angle distribution at  $Tu_v = 0$

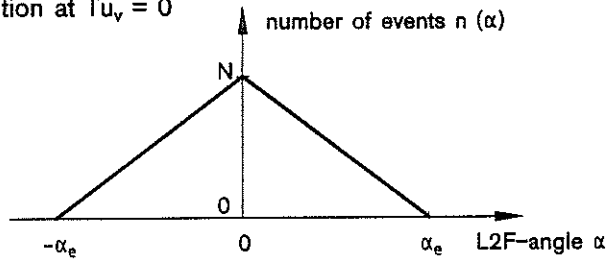


Figure 6. Angle distribution at  $Tu_v = 0$

Special case  $Tu_v = 0$

( $N$  = number of particles started at fixed angle,

$n(\alpha)$  = number of particles traversing first start then stop focus, at fixed angle) :

$$n(\alpha) = N \left( 1 - \frac{|\alpha|}{\alpha_e} \right) ; \quad \alpha_e = \frac{d}{s}$$

From such an angle distribution the variance of the angle can be determined:

$$\overline{\alpha^2} = \frac{\int_{-\alpha_e}^{\alpha_e} \alpha^2 n(\alpha) d\alpha}{\int_{-\alpha_e}^{\alpha_e} n(\alpha) d\alpha} = \frac{2}{\alpha_e} \int_0^{\alpha_e} \alpha^2 \left( 1 - \frac{\alpha}{\alpha_e} \right) d\alpha = \frac{1}{6} \left( \frac{d}{s} \right)^2$$

That means our device would measure the above computed variance of the flow angle, whereas the real flow would have the variance zero. As a result of the numer-

ical simulation it can be shown that the measured turbulence degree may be corrected at any turbulence degree by changing equation (4) on page 8:

$$\sigma_v^2 = \bar{c}^2 \left[ \overline{\sin^2 \alpha'} - \frac{1}{6} \left( \frac{d}{s} \right)^2 \right] \quad (5)$$

**Height of angle distribution as a function of turbulence degree**

Instead of determining the turbulence degree  $Tu_v$  from the angle distribution (or the 2D (u,v)-distribution), which makes a correction necessary according to the previous chapter, it is also possible to gain a functional relationship between  $Tu_v$  and the height of the angle distribution. This has already been described by Decuypere et al [4], but here the functional relationship will be explicitly given. The flow angle distribution is the measured distribution of frequency versus angle (a distribution which results from integrating the frequencies in the time-of-flight distributions at fixed angle). The measured L2F angle distributions are always rather near to a Gaussian shape. The distribution shown in Figure 2 on page 4 resembles a typical measured angle distribution.

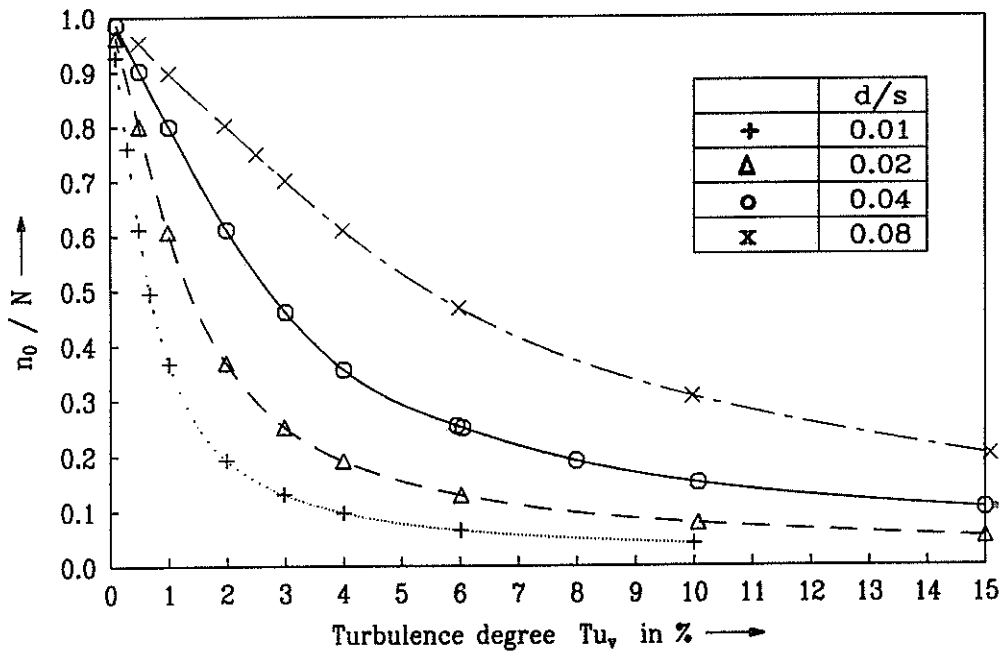


Figure 7. Height of angle distribution versus turbulence degree

$N$  = number of particles traversing the start focus at fixed angle

$n_0$  = height of angle distribution = number of particles traversing start and stop focus at angle  $\bar{\alpha}$ .

In this paper the height or amplitude of a distribution always denotes an amplitude where an eventual background level has already been subtracted. That means in all chapters apart from the chapter 'Statistical error' we look at distributions which approximate the base line zero, far from the centre. In **Figure 7** the amplitude  $n_0$  is shown as a function of  $Tu_v$  and the ratio of effective focus diameter to focus distance is a parameter. This is a result of the numerical simulation.

If the height of the angle distribution is plotted over the ratio of  $d/s$  and  $Tu_v$ , then all curves of **Figure 7** collapse to one. This is shown in **Figure 8**, where the results of the numerical simulation in the case of 'high turbulence' are plotted.

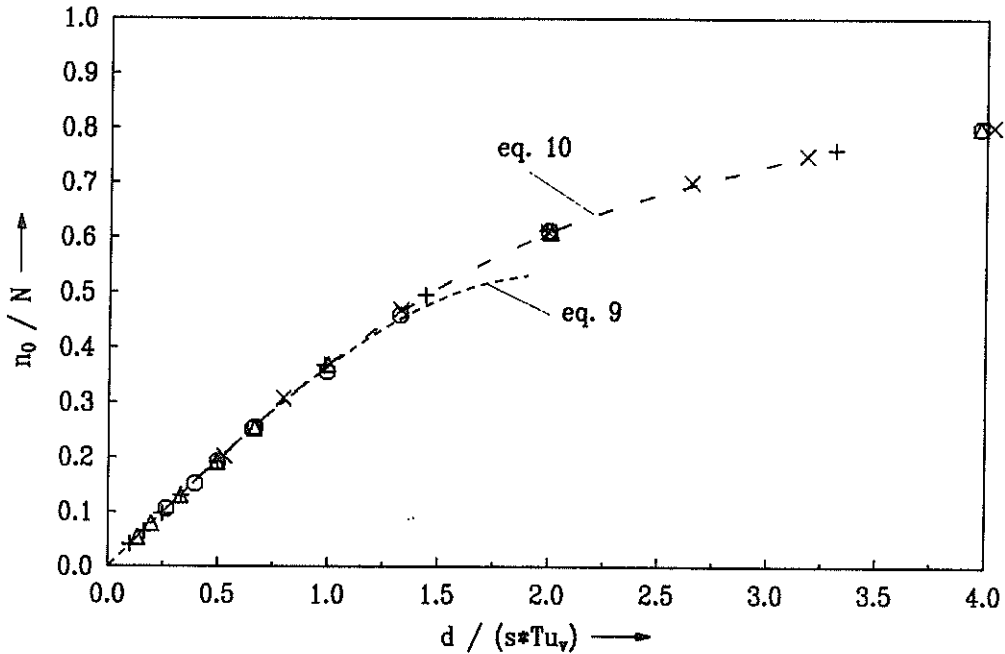


Figure 8. Height of angle distribution versus  $1 / Tu_v$ .

It is not difficult to get an analytic solution for the curve of **Figure 8** in the case of 'high turbulence degree', which means here  $Tu_v \gg d/s$ . First, it is assumed that the flow angle probability distribution has Gaussian shape:

$$\varphi(\alpha) d\alpha = \frac{1}{\sigma_\alpha \cdot \sqrt{2\pi}} \exp\left[-\frac{1}{2} \left(\frac{\alpha - \bar{\alpha}}{\sigma_\alpha}\right)^2\right]; \quad \sigma_\alpha \approx Tu_v \quad (6)$$

$\varphi(\alpha)$  is approximated in the vicinity of  $\bar{\alpha}$ :

$$\varphi(\bar{\alpha} + \alpha') \approx \varphi(\bar{\alpha}) \left[ 1 - \frac{1}{2} \left( \frac{\alpha'}{\sigma_{\alpha}} \right)^2 \right]$$

The finite diameter of the start focus is divided into three patches and the started particles are caught by the stop focus, if they remain in an angle range of  $d/s$ .

$$\frac{n_0}{N} = \frac{n(\bar{\alpha})}{N} \approx \frac{1}{3} \left[ \int_{\bar{\alpha} - \frac{d}{2s}}^{\bar{\alpha} + \frac{d}{2s}} \varphi(\alpha) d\alpha + 2 \int_{\bar{\alpha} - \frac{d}{6s}}^{\bar{\alpha} + \frac{5d}{6s}} \varphi(\alpha) d\alpha \right]$$

$$\begin{aligned} & \frac{d}{s} < Tu_v : \\ & \frac{n_0}{N} \approx \frac{d}{s \cdot Tu_v \cdot \sqrt{2\pi}} \left[ 1 - \frac{17}{216} \left( \frac{d}{s \cdot Tu_v} \right)^2 \right] \end{aligned} \quad (9)$$

In Figure 8 the analytical equation (9) is included, too. It can be seen that equation (9) is not only valid for  $d/s \ll Tu_v$ , but up to  $d/s = Tu_v$ . In Figure 8 there is furthermore included a curve showing the result of a Least Square Fit (valid for  $\frac{d}{s \cdot Tu_v} < 2.5$ ):

$$\begin{aligned} & \frac{n_0}{N} = x \cdot (1 + a x^2 + b x^3) , \text{ where} \\ & x = \frac{d}{s \cdot Tu_v \cdot \sqrt{2\pi}} ; \quad a = -0.5741; \quad b = 0.25256 \end{aligned} \quad (10)$$

In **Figure 9** the results of the numerical simulation in the case of 'low turbulence degree' are shown.

In the case of zero turbulence all particles passing the start focus also hit the stop focus (see Figure 6). When the turbulence degree in the flow takes a value above zero, more and more particles miss the stop focus at  $\alpha = \bar{\alpha}$ . Therefore the height of the angle distribution decreases rapidly. To look for an approximate analytic solution in the case of low turbulence,  $Tu_v \ll d/s$ , the situation is depicted in **Figure 10**.

We confine ourselves to particles starting in the upper half of the start cylinder, because of symmetry. At any  $y$ -value of the first focus particles start, possessing a rather narrow flow angle distribution. If the actual angle of a particle deviates from  $\bar{\alpha}$  less than  $(d/2 - y)/s$ , it will hit the stop focus.

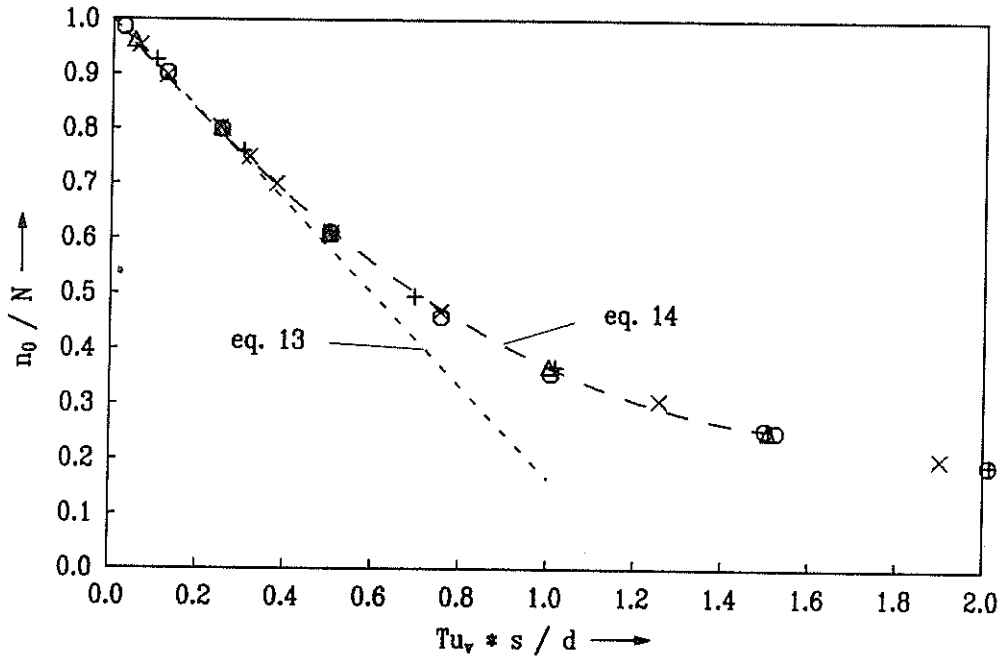


Figure 9. Height of angle distribution versus  $Tu_v \cdot s/d$

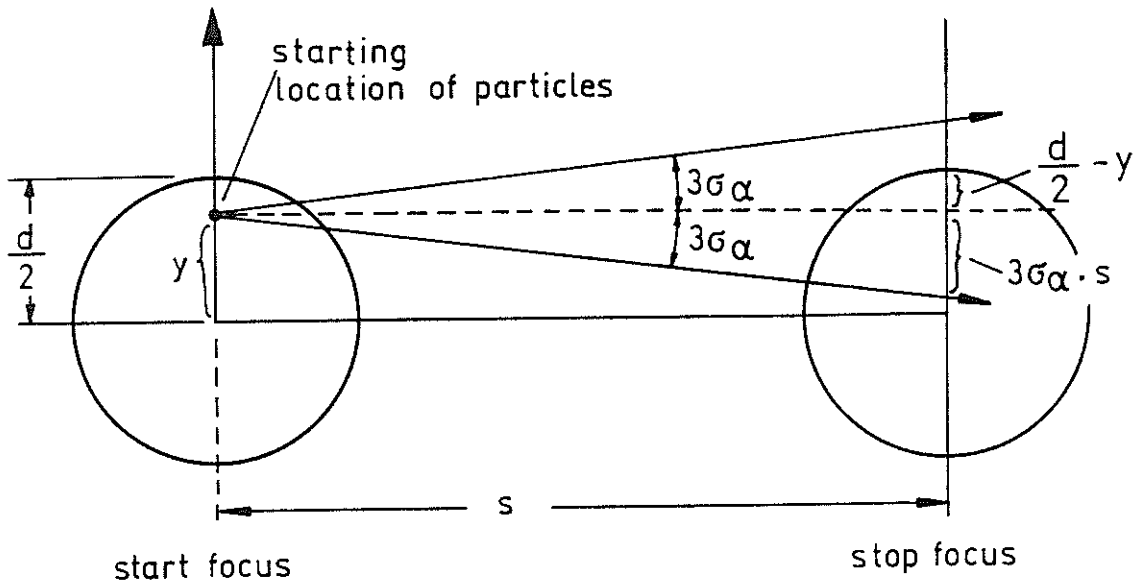


Figure 10. Measurement volume and flow angle distribution, if  $Tu_v \ll s/d$



$$\alpha' = \alpha - \bar{\alpha}; \quad \sigma_{\alpha} = Tu_v; \quad Tu_v \ll \frac{d}{s};$$

$$n_0 \approx \frac{2}{d} \int_0^{\frac{d}{2}} n(y) dy, \quad \text{where}$$

$$n(y) = N, \quad \text{if } \frac{d}{2} - y > 3\sigma_{\alpha} s, \quad \text{or} \quad (11)$$

$$n(y) = N \int_{-3\sigma_{\alpha}}^{\frac{\frac{d}{2}-y}{s}} \varphi(\alpha') d\alpha', \quad \text{if } y > \frac{d}{2} - 3\sigma_{\alpha} s$$

For simplicity, it is assumed that the flow angle probability distribution  $\varphi$  has triangular shape, but the same amplitude as the Gaussian distribution of equation (6):

$$\varphi(\alpha') d\alpha' = \frac{1}{\sigma_{\alpha} \cdot \sqrt{2\pi}} \left( 1 - \frac{|\alpha'|}{\sigma_{\alpha} \cdot \sqrt{2\pi}} \right), \quad \text{and} \quad (12)$$

$$\varphi(\alpha') d\alpha' = 0, \quad \text{if } |\alpha'| > \sigma_{\alpha} \cdot \sqrt{2\pi}$$

The final result is:

$$\frac{d}{s} \gg Tu_v: \quad \frac{n_0}{N} \approx 1 - \frac{\sqrt{2\pi}}{3} \frac{s \cdot Tu_v}{d} \quad (13)$$

In Figure 9 the analytical equation (12) is included. In Figure 9 there is furthermore included a curve showing the result of a Least Square Fit (valid for  $\frac{s \cdot Tu_v}{d} < 1.4$ ):

$$\frac{n_0}{N} = 1 - 0.9020 \frac{s \cdot Tu_v}{d} + 0.2698 \left( \frac{s \cdot Tu_v}{d} \right)^2 \quad (14)$$

As the valid regions, belonging to the equations (10) and (14) overlap, it is possible to compute the height of the angle distribution for any turbulence degree. The above analysis always implicitly supposed to have a symmetric or even Gaussian angle distribution. This is true for isotropic turbulence. Nevertheless, from some examples of the numerical simulation it followed that the above results seem to be applicable even for non-isotropic turbulence, if really the amplitude of the angle distribution is taken, not the value at  $\alpha = \bar{\alpha}$ . In the next chapter it will be demonstrated that the unknown parameter  $d/s$  can also be determined from the measured angle distribution, so no extra calibration is necessary.

***Sum of events in the angle distribution***

- N = number of particles traversing the start focus at a fixed angle
- $n_i$  = number of particles traversing start and stop focus at the  $i$ th angle
- $m$  = number of angles during a L2F-measurement,  $m > 2$
- $\alpha_i$  =  $i$ th L2F angle (in radians)
- $\Delta\alpha = \alpha_i - \alpha_{i-1}$

Supposition :

During a L2F-measurement the angle distribution is fully scanned,

$|\alpha_m - \alpha_1| > \text{Max} ( 6 \sigma_\alpha, 2 \frac{d}{s} )$ . This condition means: The width of the measured angle distribution is either governed by the width of the flow angle distribution ( $6 \sigma_\alpha$ ) or by the L2F device angle  $2d/s$ , but the L2F angle range should be larger, if one wants to apply the following formula. Furthermore, also the choice of the L2F angles  $\alpha_i$  should be such that the flow angle distribution is fully scanned. This implies that of course the mean angle  $\bar{\alpha}$  has to be included and the number of L2F angles,  $m$ , should be large enough.

$\sum_{i=1}^m n_i = \frac{d}{s} \frac{(m-1) \cdot N}{ \alpha_m - \alpha_1 } = \frac{d}{s} \frac{N}{\Delta\alpha} \tag{15}$
--

The above equation enables us to compute the unknown parameter  $d/s$  from an L2F measurement. Of course the basic assumptions of the numerical simulation, stated earlier, must be valid. Up to now these assumptions have not been checked experimentally, but it should be done in the future.

As the minimum angle range  $|\alpha_m - \alpha_1|$  is dependent on turbulence degree (if  $3 \sigma_\alpha > d/s$ ; remember  $\sigma_\alpha \approx Tu_v$ ), it follows from the above formula that for higher turbulence, in order to get the same number of succesful events in the measured angle distribution, you have to increase either  $d/s$  or the number of angles,  $m$ , or the number of particles started per angle,  $N$ . The only way to achieve this without increasing measurement time is to increase  $d/s$  (see Schodl and Förster [5]). As in the up to now installed L2F devices there is normally no possibility to change the distance of the focus, it is advisable to have a ratio of  $d/s$  as large as possible from other reasons. One should not fear a large  $d/s$  at moderate to small turbulence degrees, as according to Figure 7, even at the the ratio  $d/s = 0.08$  the dependence of the amplitude  $n_0$  on turbulence degree is rather strong, which means that there is a possibility to detect small turbulence degrees.

## ***Conclusion***

In the paper some important measurement errors intrinsic to L2F measurements have been numerically and analytically investigated. These are:

- Statistical error of distributions with background noise at the baseline.
- Evaluation errors caused by using integrated distributions which have been produced by integrating 2D distributions in the polar system.
- Error in the measured turbulence degree caused by the finite diameter of the focus.

The L2F measurement time may be reduced by measuring only the central part of the flow angle distribution and especially by using L2F optics with a small focus distance  $s$  i.e. a large ratio of focus diameter to distance,  $d/s$ . To be able to measure small turbulence degrees also in the case of large  $d/s$ , following relations have been quantitatively determined:

- The dependence of the height of the angle distribution on turbulence degree and  $d/s$ .
- The sum of events in the angle distribution i.e. the probability of successfully hitting start and stop focus as a function of the measurement parameters.

As the above mentioned relations have been derived only numerically and partly analytically, there is still a strong need to check the relations by experiment.

## ***References***

- [1] Schodl, R.  
*A Laser-Two-Focus (L2F) Velocimeter for Automatic Flow Vector Measurements in the Rotating Components of Turbomachines*  
J. Fluid Eng., Vol 102, pp. 412-419, 1980
- [2] Kost, F.  
*Three Dimensional Transonic Flow Measurements in an Axial Turbine with Conical Walls*  
ASME paper 92-GT-61, International Gas Turbine and Aeroengine Congress, Cologne, Germany, 1992
- [3] Humphreys, W.M.; Hunter, W.W.  
*Estimating Laser Transit Anemometry Noise Performance Capabilities*  
ICIASF 1989 Record, Göttingen, 1989

- [4] Decuypere, R.; Riethmuller, M.L.; Leblanc, R.; Mercier, V.  
*Boundary Layer Transition Detection in Transonic Flows by Laser Transit Velocimetry*  
 10th Symposium on "Measuring Techniques for Transonic and Supersonic Flow in Cascades and Turbomachines", VKI, Brussels, September 17-18, 1990
- [5] Schodl, R.; Förster, W.  
*A New Multi Colour Laser Two Focus Velocimeter for 3-Dimensional Flow Analysis*  
 ICIA SF 1989 Record, Göttingen, 1989
- [6] Bobroff, N.  
*Position measurement with a resolution and noise-limited instrument*  
 Rev.Sci.Instrum. 57 (6), June 1986

### *Appendix: Distortion of a focus by a plane window*

It is known that a focussed light beam will be distorted when it passes a plane window. When the light beam axis deviates strongly from the vertical on the window this distortion is especially marked.

It is assumed that without a glass window the light beam is perfectly focussed. Then the light beam is a cone with the cone angle  $\delta$ . A rectangular coordinate system is chosen such that the focus of the undisturbed beam is at the origin. Now a plane glass window of thickness  $t$  will be inserted. The light beam axis and the vertical on the window include an angle  $\alpha$  (see **Figure 11**). The x-direction of the coordinate system coincides with the vertical on the window, y- and z-axis are parallel to the plane of glass and the y-axis is furthermore located in the plane of beam axis and vertical of the window.

After the insertion of the glass pane a single light ray can be described by following formulas ( $\alpha'$  = angle included by light ray and glass vertical in the xy-plane;  $\delta'$  = angle between light ray and xy-plane).

Light ray above the pane of glass:

$$\begin{aligned} y &= x \tan \alpha' \\ z &= x \tan \delta' / \cos \alpha' \end{aligned} \quad (16)$$

Light below the pane of glass (thickness  $t$ , refractive index  $n$ ):

$$\begin{aligned} y &= (x + t) \tan \alpha' - \frac{t \sin \alpha' \cos \delta'}{\sqrt{n^2 - 1 + \cos^2 \alpha' \cos^2 \delta'}} \\ z &= \frac{(x + t) \tan \delta'}{\cos \alpha'} - \frac{t \sin \delta'}{\sqrt{n^2 - 1 + \cos^2 \alpha' \cos^2 \delta'}} \end{aligned} \quad (17)$$

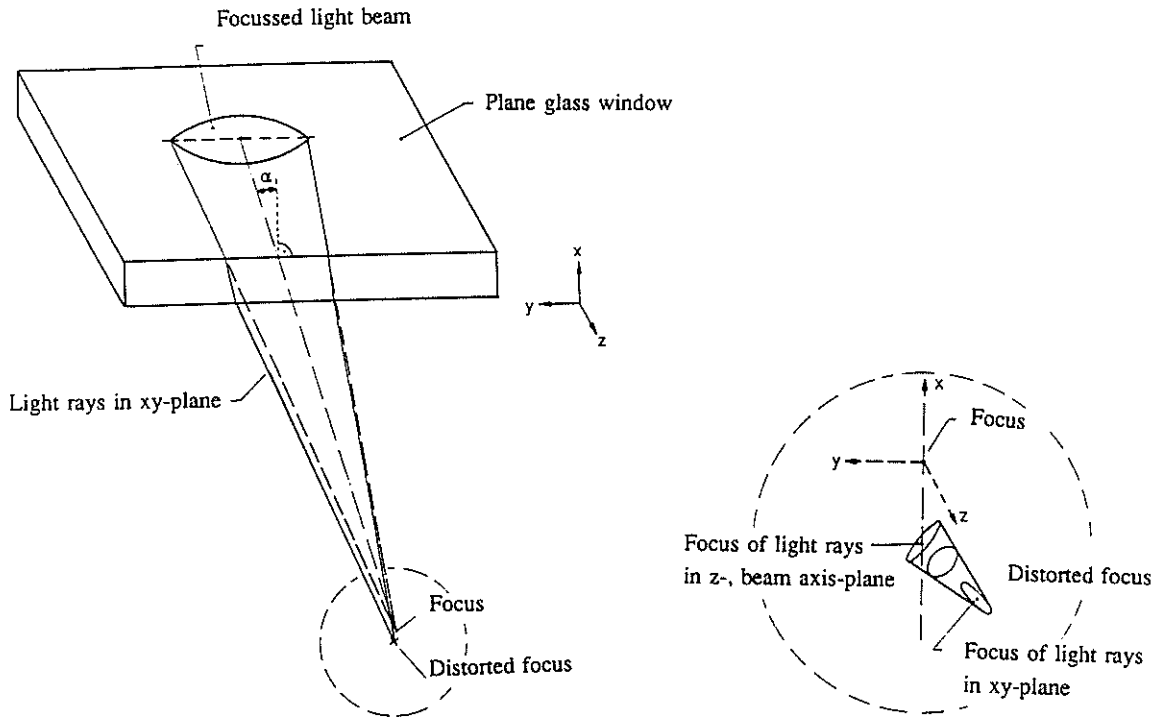


Figure 11. Light rays

After inserting the glass window any two light rays will no longer intersect. But using the L2F optics the cone angle  $\delta$  of the light beam is relatively small (in our case  $\delta = 7,2^\circ$ ;  $\delta/2 = 0,06$  rad). Therefore it is sufficient to inspect light rays which are near to the axis of the beam. The angle  $\alpha$  of light beam and vertical on the window shall not be neglected.

One gets following equations for the point of intersection of the light rays in the xy-plane ( $\delta' = 0$ ,  $\alpha' = \alpha \pm \epsilon$ ,  $\epsilon \ll 1$ ):

$$\frac{x+t}{t} = \frac{n^2 \cos^3 \alpha}{(n^2 - \sin^2 \alpha)^{3/2}}$$

$$\frac{y}{t} = \frac{(1 - n^2) \sin^3 \alpha}{(n^2 - \sin^2 \alpha)^{3/2}} \quad (18)$$

$$z = 0$$

In contrast to the above results one gets different formulas for the point of intersection of two light rays lying in the plane of beam-axis and z-axis, outside the xy-plane ( $\alpha' = \alpha$ ,  $\delta' = \pm \epsilon$ ):

$$\frac{x + t}{t} = \frac{\cos \alpha}{\sqrt{n^2 - \sin^2 \alpha}} \quad (19)$$

$$y = 0, \quad z = 0$$

The different coordinates of the two new focus which result from the equations according to (18) and (19) denote a distortion (an astigmatism). The shift of the original focus is not a problem, but the distortion cannot be corrected (at least not easily) and it may lead to a strong deterioration of the signal.

According to Figure 11 the result may be interpreted in the following way: Somewhat nearer to the original focus the light rays of the beam-axis, z-axis plane intersect. An elliptic focus exists at that point. A little bit more distant from the x-axis the light rays in the xy-plane intersect. Here again the focus is elliptic. In between the two intersection locations according to (18) and (19) the 'focus' is round but much thicker than the original one. As a characteristic length of the distortion one may take the distance of the two intersection locations according to (18) and (19). This characteristic length is plotted in **Figure 12**.

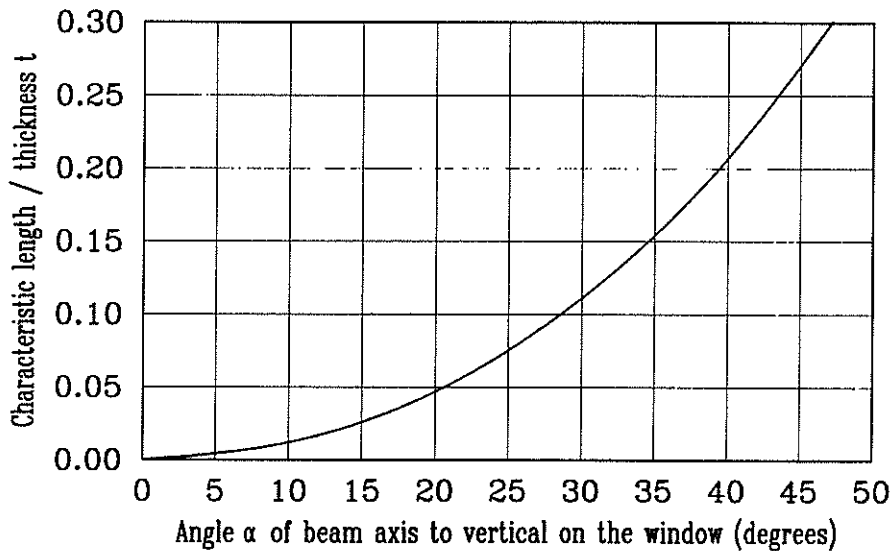


Figure 12. Characteristic length of distortion of the focus by a plane window ( $n = 1.51$ )

From the above equations one may also compute the direction of the distortion. It results that the direction of the distortion is in the direction of the new beam axis. That is why the distance,  $s$ , of the L2F start- and stop focus remain the same after insertion of the plane glass window. The latter result could be confirmed experimentally. To correct the distortion a cylinder lens would be necessary.